Hierarchical accumulation of RyR post-translational modifications drives disease progression in dystrophic cardiomyopathy.

Sergii Kyrychenko[1*], Eva Poláková[1*#], Chifei Kang[1], Krisztina Pocsai[1], Nina D. Ullrich[2], Ernst Niggli[2] and Natalia Shirokova[1].

From the Department of Pharmacology and Physiology[1], UMDNJ– New Jersey Medical School, Newark 07103, NJ, USA and the Department of Physiology[2], University of Bern, CH-3012 Bern, Switzerland.

*Sergii Kyrychenko and Eva Poláková contributed equally to this work.

[#]Eva Poláková current address: Department of Pharmacology & Systems Therapeutics, Mount Sinai School of Medicine, New York 10029, NY, USA

Running title: cellular phenotype of cardiac dystrophy

Key words: Dystrophic cardiomyopathy, excitation-contraction coupling, ryanodine receptor, Ca^{2+} signals

Total word count: 6320

Address correspondence to: N. Shirokova, Department of Pharmacology and Physiology, University of Medicine and Dentistry – UMDNJ, 185 S. Orange Ave., Newark 07103, NJ, USA. E-mail: nshiroko@umdnj.edu. Ph: (973) 972 8877. Fax: (973) 972 7950.

Aims: Duchenne muscular dystrophy (DMD) is a muscle disease with serious cardiac complications. Changes in Ca^{2+} homeostasis and oxidative stress were recently associated with cardiac deterioration, but the cellular pathophysiological mechanisms remain elusive. We investigated whether the activity of ryanodine receptor (RyR) Ca^{2+} release channels is affected, whether changes in function are cause or consequence and which post-translational modifications drive disease progression.

Methods and Results: Electrophysiological, imaging and biochemical techniques were used to study RyRs in cardiomyocytes from *mdx* mice, an animal model of DMD. Young *mdx* mice show no changes in cardiac performance, but do so after ~8 months. Nevertheless, myocytes from *mdx* pups exhibited exaggerated Ca^{2+} responses to mechanical stress and "hypersensitive" excitation-contraction coupling, hallmarks of increased RyR Ca^{2+} sensitivity. Both were normalized by antioxidants, inhibitors of NAD(P)H oxidase and CaMKII, but not by NO-synthases and PKA antagonists. SR Ca^{2+} load and leak were unchanged in young *mdx* mice. However, by the age of 4-5 months and in senescence, leak was increased and load was reduced, indicating disease progression. By this age, all pharmacological interventions listed above normalized Ca^{2+} signals and corrected changes in ECC, Ca^{2+} load and leak.

Conclusions: Our findings suggest that increased RyR Ca^{2+} sensitivity precedes and presumably drives the progression of dystrophic cardiomyopathy, with oxidative stress initiating its development. RyR oxidation followed by phosphorylation, first by CaMKII and later by PKA, synergistically contributes to cardiac deterioration.

1. Introduction.

Cytoskeletal remodeling often accompanies cardiac hypertrophy and failure[1]. Dystrophinopathies represent a unique group of diseases in which the cytoskeletal disarray is not only a consequence but also the cause of the disease. They result from mutations in the dystrophin gene[2]. Duchenne muscular dystrophy (DMD) is among the most severe forms of dystrophy. Cardiac manifestations of the disease are present in the majority of adolescent boys with DMD. About 20% of the patients suffer from ventricular dysfunctions and arrhythmias that ultimately lead to heart failure or sudden cardiac death[3]. The most commonly used animal model of DMD is the *mdx* mouse, which lacks dystrophin. *Mdx* mice develop dilated cardiomyopathy over an eight-month period[4,5]. By that age they also show electrocardiographic and MRI abnormalities and develop sustained ventricular tachycardia when challenged with isoproterenol[6].

The cellular pathology of the failing heart often shows impaired intracellular Ca^{2+} homeostasis, including abnormal excitation-contraction (EC) coupling[7]. It is well described that at different stages of dystrophic cardiomyopathy its cellular phenotype exhibits augmented intracellular Ca^{2+} responses (i.e. a burst of Ca^{2+} sparks and waves) to mechanical stress[8-10], hypersensitive EC-coupling [11], increased Ca^{2+} leak from the sarcoplasmic reticulum (SR) and reduced SR Ca^{2+} load[6]. These features clearly point to modifications in intracellular Ca^{2+} cycling and suggest elevated activity of Ca^{2+}-induced Ca^{2+} release (CICR) from the SR via ryanodine receptor (RyR). As underlying causes, several and probably not mutually exclusive mechanisms of RyRs sensitization have been considered. They include oxidative[9] and nitrosative[6] post-translational modifications of RyRs as well as their phosphorylation by PKA[12]. However, a causal links between these modifications and alterations of RyR function, development of cellular abnormalities and progression of dystrophic cardiomyopathy have not yet been established clearly.

3

The aim of this study was to define the interactions among several cellular pathomechanisms that converge to a common end-point – they ultimately all sensitize or even hypersensitize the CICR machinery, in particular the RyRs. In addition, we wanted to determine whether RyR hypersensitivity to Ca^{2+} precedes and therefore possibly underlies the progression of this disease. We found that gradually developing and additive modifications of RyRs provoke the degradation of cardiomyocyte function that may ultimately result in cardiac failure in muscular dystrophy.

2. Methods

For additional information on methods see Supplementary material online.

2.1. Cell isolation

All experiments conformed with the NIH Guide for the Care and Use of Laboratory Animals published by the US National Institute of Health (NIH publication, 8th Edition, 2011) and were approved by the Institutional Animal Care and Use Committee of the New Jersey Medical School, USA and by the State Veterinary Office of Bern, Switzerland. C57BL10 mice (wild-type, WT) and dystrophin-deficient *mdx* (C57BL/10ScSn-*mdx*) mice at the age of 1 (young), 3-4 (adult) and 12-15 months (senescent) were used in this study. Animals were purchased from the Jackson Laboratory. Ventricular myocytes were enzymatically isolated as previously described[13]. Briefly, mice were heparinized (5,000 U/kg), anesthetized with sodium pentobarbital (100 mg/kg), and checked to ensure absence of movement, flexor and pedal reflexes. Hearts were then quickly removed, mounted on a Langendorff apparatus and perfused with a solution containing collagenase and protease. Ventricles were cut into small pieces from which cells dissociated with time. Myocytes were used for experiments within 5 hours after isolation.

2.2. Cellular experiments

Changes in cytoplasmic $[Ca^{2+}]$ and production of reactive oxygen species (ROS) were monitored with fluorescent indicators fluo-3 AM (5 µM) and 5-(and-6)-chloromethyl-$2',7'$-dichlorodihydrofluorescein diacetate (CM-H$_2$DCFD, 20 µM), respectively and a laser-scanning confocal microscope (Bio-Rad, Radiance 2000) in *XY*-scan mode at the rate of 0.5 Hz. Dyes were excited with the 488 nm line of an Argon laser. The emitted light was collected above 500 nm. SR Ca^{2+} leak was estimated as described in[14]. Cells were paced at 1 Hz in external control

solution to obtain steady-state levels of SR Ca^{2+} load, and starting from the last five beats, $[Ca^{2+}]_i$ was recorded in the line-scan mode (500 lines/s). After pacing, external solution was rapidly switched to Na^+ and Ca^{2+}-free solution for 15 s to stop Ca^{2+} influx and to inhibit Ca^{2+} removal via the NCX and thus, to avoid Ca^{2+} overload or Ca^{2+} unloading of the cells. Addition of tetracaine (1 mM, 15 s) eliminated RyR-mediated diastolic Ca^{2+} leak, leading to a rapid decrease in $[Ca^{2+}]_i$ proportionally to the leak. The peak of the caffeine-induced Ca^{2+} transient measured after tetracaine washout (10 mM caffeine, 2 s) was used to estimate SR load. Membrane currents were recorded using the whole cell patch-clamp technique with an Axopatch 200B amplifier (Axon Instruments). Cells were voltage clamped using low-resistance (1.5–3 MΩ) borosilicate glass micropipettes filled with pipette solution which contained (in mL): 120 CsAsp, 8 NaCl, 20 tetraethylammonium (TEA)-Cl, 5.5 $MgCl_2$, 4 KATP, 5 HEPES, and 0.1 K_5-fluo-3. pH was adjusted to 7.2 with CsOH and osmolarity was 305 mOsm. All experiments were carried out at room temperature, which may represent an experimental limitation of our studies.

2.3. Phosphorylation and oxidation of RyRs

Phosphorylation status of RyRs at Ser-2808 (PKA) and Ser-2814 (CaMKII) was assessed with antibodies purchased from Badrilla (UK) and CaMKII expression was evaluated with antibodies donated by Dr. M.E. Anderson (University of Iowa) using standard procedures[15]. Briefly, mouse ventricular tissue was collected and sonicated in the radio-immunoprecipitation assay (RIPA) lysis buffer. 40 µg of protein lysate per sample was denatured in 4X SDS-PAGE sample loading buffer. Proteins were separated by electrophoresis in 4% (for RyR2) and 10% (for CaMKII) respectively SDS-polyacrylamide gel, transferred to nitrocellulose membrane (Bio-Rad, CA) at 15V for 16-18 h at 4^0C (for RyR2) and at 90V for 15 h at 4^0C (for CaMKII), blocked with 1% BSA in TRIS buffered saline and Tween (TBS: 20mM TRIS-HCl, 200mM NaCl, 0.6% tween 20, pH 7.5) for 1 hour and probed for proteins of interest.

The content of free thiols was determined using a monobromobimane (mBB, Calbiochem, USA) assay[16]. Isolated cardiomyocytes were permeabilized and incubated with 1 mM of mBB for 1 hour in a dark room. The proteins were separated in 4-15% TGX SDS-gels (Bio-Rad, CA) and imaged with UV excitation (360 nm). Total RyR2 was determined from Coomassie blue staining of gels run in parallel and confirmed by western blotting with anti-RYR2 (Thermo Scientific, MA) and Mass Spectrometry at UMDNJ core facility.

2.4. Statistics

Results are shown as mean ± standard error (SEM). All data sets contain results from a minimum of three mice (n on the figures indicates the number of cells studied with imaging and electrophysiological techniques or the number of tissue samples in biochemical experiments). Statistical significance was evaluated by Student's t-test. A P-value of <0.05 was considered significant.

3. Results

3.1. RyRs are already hypersensitive to activation by Ca^{2+} in myocytes from young *mdx* mice

At the age of one month dystrophic mice do not exhibit any signs of cardiac disease. However, 74% of apparently normal dystrophic cardiomyocytes exhibited exaggerated intracellular Ca^{2+} signals (Ca^{2+} waves and sparks) in response to a mechanical challenge applied as mild hypo-osmotic shock at rest. In contrast, intracellular Ca^{2+} transients in WT cells were minimal and detected only in 20% of myocytes (*Figure 1A*). Since the extent of Ca^{2+} influx is only slightly larger in *mdx* myocytes[9,17], this observation was taken as a strong indication of increased Ca^{2+} sensitivity of RyRs in young dystrophic hearts.

In order to obtain more detailed insight into RyR function, we measured Ca^{2+} currents (I$_{Ca}$), corresponding Ca^{2+} transients and determined the gain of EC-coupling in patch-clamped cells. EC-gain reflects the efficiency of signal transduction between L-type Ca^{2+} channels and RyRs. The gain is calculated as the ratio of Ca^{2+} transient amplitude to the peak of corresponding I$_{Ca}$. When cells were superfused with a normal experimental solution, containing 1.8 mM Ca^{2+}, we found no significant difference in the amplitudes of I$_{Ca}$, Ca^{2+} transients and values of EC-coupling gain between the two groups of cells within a range of test voltages (-25 to +50 mV). This observation was in agreement with our previous findings in myocytes from more mature animals[11]. Then we repeated the analysis of Ca^{2+} transients and I$_{Ca}$ at the lowest test voltage (-25 mV), but under conditions that challenge the fidelity of EC-coupling mechanisms - reduced Ca^{2+} concentration in the superfusion solution (0.5 mM instead of 1.8 mM[11,18]. As a result, the I$_{Ca}$ and Ca^{2+} transient amplitudes were significantly decreased in all cardiomyocytes. However, the corresponding reduction in the amplitude in cytosolic Ca^{2+} transient was significantly less in *mdx* cells compared to WT, while the amplitude of I$_{Ca}$ was affected to the same extent (*Figure 1B*, middle panes). This corresponds to a significantly

smaller reduction in EC-coupling gain in dystrophic cells (*Figure 1B*, right panels). Thus, in contrast to young WT myocytes, SR Ca^{2+} release in *mdx* cells exhibited a surprising resistance to the reduction in I_{Ca} trigger, revealing a hypersensitivity in EC-coupling that is an additional indication of an increased sensitivity of RyRs to Ca^{2+}.

An abnormal Ca^{2+} sensitivity of the RyRs could manifest itself as an elevated SR Ca^{2+} leak, resulting in a decreased Ca^{2+} content of the SR, reduced SR Ca^{2+} release and impaired cellular contractility. Such changes were previously observed in 3-4 month old *mdx* myocytes and were attributed to hyper-phosphorylation of RyRs by PKA[19]. We compared the transient Ca^{2+} leak from the SR as well as the resting SR Ca^{2+} load using a method developed in[14]. The SR of intact cardiomyocytes was loaded with Ca^{2+} by a train of field stimulations. Subsequently, the SR Ca^{2+} leak was estimated from the decrease in resting $[Ca^{2+}]_i$ following addition of the RyR blocker tetracaine. The peak of a caffeine-induced Ca^{2+} transient after tetracaine washout was used to estimate the SR Ca^{2+} load. No statistically significant increase in the transient SR Ca^{2+} leak was observed in myocytes from young mice, suggesting that the detection of such changes requires more severe modifications in RyRs functions (see below). The somewhat higher SR Ca^{2+} content in *mdx* myocytes may result from the slightly elevated trans-sarcolemmal Ca^{2+} influx in these cells[9,17,20].

3.2. Hypersensitivity of RyRs is driven by oxidation in young *mdx* myocytes

There is a number of post-translational modifications that may contribute to the increased sensitivity of RyR activation by Ca^{2+}. Oxidation, nitrosation and phosphorylation are among them. Oxidative modification of RyRs was one of the first proposed mechanisms contributing to an impaired Ca^{2+} homeostasis of dystrophic cardiomyocytes[9,21]. Moreover, an increased activity of plasmalemmal NAD(P)H oxidase (NOX) was identified to be a major source of oxidative stress in dystrophic cardiomyopathy[9,10,21]. Here we tested whether oxidative stress modifies RyR functions already in very early stages of the disease. Four groups of experiments were

performed: we 1) compared the extent of ROS production in WT and *mdx* cardiomyocytes with confocal microscopy and CM-H$_2$DCFDA; 2) assessed the oxidation and phosphorylation status of RyRs using mBB assays and phospho-specific antibodies against RyR PKA and CaMKII sites Ser-2808 and Ser-2814; 3) evaluated the oxidative status of CaMKII with antiserum against oxidized Met281/282 residues; and 4) tested whether scavengers of ROS, inhibitors of NOX, CaMKII, PKA and various isoforms of nitric oxide synthase (eNOS, nNOS and iNOS) "normalize" hypersensitive Ca^{2+} responses to osmotic shock and EC-coupling in dystrophic myocytes.

To assess oxidative stress, myocytes isolated from WT and *mdx* mice were identically loaded with CM-H$_2$DCFDA. CM-H$_2$DCFDA is hydrolyzed to DCFH in the cell, and DCFH is oxidized to form the highly fluorescent DCF compound in the presence of an appropriate oxidant. It should be noted that, as many other ROS indicators, DCF is not exclusively selective to detect ROS, but also some reactive nitrogen species (RNS). DCF-related fluorescence was followed for ~3 min under resting conditions (*Figure 2A*). The slope of the averaged DCF signal largely reflects the rate of cellular ROS production. It was significantly greater in *mdx* cells. Another way to assess the redox state of the cytosol is to normalize resting DCF fluorescence (F$_0$) to the signal after addition of 10 mM H$_2$O$_2$ (F$_{max}$) The relative increase of fluorescence after addition of H$_2$O$_2$ was significantly smaller in *mdx* myocytes, also indicating an increased resting ROS/RNS level in dystrophic hearts of young animals. Purified cardiac RyR tetramer contains multiple free cysteines[22] which can be readily oxidized. The content of free thiols in RyRs was determined with the mBB technique. Relative content of free thiols in RyR was ~70% greater in WT, suggesting that oxidative stress in dystrophic cells resulted in oxidation of RyRs (*Figure 2B*).

RyRs are also predisposed to phosphorylation by both CaMKII and PKA. Moreover, CaMKII itself is susceptible to oxidative activation[23]. Based on our data, the enzyme is expected to be more actively involved in *mdx* cardiomyocytes, as the amount of oxidized enzyme

increased about 2-fold in dystrophic cells (*Figure 2C*). We assessed the phosphorylation status of RyRs with phospho-specific antibodies against Ser-2814 (putative phosphorylation site for CaMKII) and Ser-2808 (proposed site for PKA phosphorylation). These experiments indicate that CaMKII-, but not PKA-mediated phosphorylation, also contribute to the early cellular dysfunctions in dystrophic cardiomyopathy (*Figure 2D*).

To further evaluate the contribution of each particular post-translational RyR modification, a set of functional studies with various pharmacological tools was carried out. *Figure 2E* illustrates that the reducing agent 2-mercaptopropionyl glycine (MPG, 1 mM), inhibitors of NOX (apocynin, 0.5 mM and diphenylene iodonium (DPI), 10 μM) and CaMKII (K-93, 5 μM and Autoctamide-2 Related Inhibitory Peptide (AIP), 2.5 μM) reversibly inhibited intracellular Ca^{2+} responses to osmotic shock and normalized EC-coupling in *mdx* cells. In contrast, various PKA inhibitors (H89, 5 μM, KT5720, 2 μM and PKA inhibitory peptide (PKI), 5 μM) as well as inhibitors of nNOS, eNOS and iNOS (S-methyl-L-Thiocitrulline (SMLT), 10 μM and 1400W, 100 nM, respectively) had no significant effect on the intracellular Ca^{2+} signals in *mdx* myocytes from young animals (see *Table 1S* for details). Please note that after testing a broad range of inhibitors of PKA and CaMKII in the experiments with osmotic shock, we used only the more specific inhibitory peptides of kinases (AIP and PKI) in subsequent work. Right panel in *Figure 2D* shows that "hypersensitive" gain of EC-coupling in dystrophic cells was also normalized by reducing factors and inhibitors of NOX and CaMKII but was not affected by inhibitors of PKA or NOS. These results are in agreement with biochemical studies by us and others[6,19] that did not reveal changes in PKA-phosphorylation or nitrosative status of RyRs in very young *mdx* hearts. Taken together, the findings presented so far are consistent with the hypothesis that oxidative stress due to an increased production of ROS by NOX drives the cellular pathology of cardiac dystrophy at very early stages of the disease.

3.3. The progression of cellular pathology in cardiac dystrophy

Data presented above suggest that cellular abnormalities in isolated dystrophic cardiomyocytes clearly precede the first clinical signs of cardiomyopathy[4,5]. Here we followed up on the progression of the cellular phenotype of the disease to the age where heart dysfunction becomes prominent. Ventricular myocytes were isolated from 3-4 and 12-15 month old animals. Similar to the experiments shown above, intracellular Ca^{2+} responses to mild osmotic shock, EC-coupling, SR Ca^{2+} leak and load were examined. Data are summarized in *Figure 3*, which also includes some results from one month old mice adapted from *Figure 1* for comparison. With the progression of the disease, more *mdx* cardiomyocytes exhibited excessive intracellular Ca^{2+} responses to osmotic shock (74%, 90% and 95% for the three age groups studied, respectively). EC-coupling became extremely hypersensitive at the age of 3-4 month (just before the clinical onset of the disease) but sensitivity remained relatively high in the senescent animals. Contrary to cells from young mice, the transient SR Ca^{2+} leak significantly increased in *mdx* cells isolated from 3-4 month old animals. This was associated with a tendency towards reduced SR Ca^{2+} content. However, a significant decrease in the SR Ca^{2+} load was only recorded in very old animals that had already developed cardiac myopathy. This decrease is at least partly responsible for a reduced resistance of the EC-coupling gain to challenges when compared to younger animals (i.e. reducing $[Ca^{2+}]$ in the external solution and applying a small test depolarization, *Figure 3 B*).

We also carried out experiments similar to those illustrated in *Figure 2*. It seems that by the age of 3-4 months (just before the appearance of clinical signs of cardiac dystrophy) several post-translational modifications additively enhance RyR function resulting in increased SR Ca^{2+} leak, reduced SR Ca^{2+} content and consequently impaired force production by the individual myocytes. In cells from *mdx* mice older than 3 months activation of NOS and PKA also seems to contribute to the hypersensitivity, possibly further aggravating the disease at later stages. A variety of pharmacological tools supports this conclusion as they not only normalized intracellular Ca^{2+} responses during mechanical stress and EC-coupling in older animals (*Figure*

4 A and *B*) but also significantly reduced intracellular Ca^{2+} leak in senescent mice (*Figure 4 C*).

4. Discussion

Most cardiac diseases are accompanied by substantial remodeling of the heart tissue, also on cellular and molecular level[24]. Depending on the cause of the illness and the particular pathophysiology, various adaptive remodeling mechanisms can initially compensate for the functional impairments. Unfortunately, some of these initially beneficial processes can become maladaptive with time and during progression of the illness, finally aggravating rather than improving the cardiac condition. This interplay between 1) defects causing a cardiac disease and 2) the remodeling mechanisms that try to maintain function leads to a very complex situation. This complexity makes it extremely challenging to unravel the causal disease mechanisms and to comprehend the evolution of the disease. However, such an understanding would greatly facilitate the development of new therapies and the identification of new drug targets.

One possible strategy to gain insight into the interplay between causal and adaptive alterations of cardiac muscle is to follow the disease progression over longer periods of time. This approach is based on the rationale that causal changes can presumably be identified from the beginning of the disease, even before the pathology becomes manifest, while adaptive and maladaptive processes will develop at later stages only.

Based on this reasoning we carried out the present study, examining disease progression in dystrophic cardiomyopathy. Because of their slowly developing cardiac phenotype *mdx* mice are a useful model for studies of the progression of DMD that can help to identify the cellular sequence of events leading from the genetic defect (lack of functional dystrophin) to the onset of cardiac disease. Hearts of 1-2 month old *mdx* mice seem to have normal morphology, left ventricular function and echocardiograms. First signs of cardiac disease, such as reduced left ventricular filling, ejection fraction and ejection rate, are seen only in 3 month old animals. These changes are more prominent and can be detected earlier in the

14

right ventricle. By 8 months of age, hearts from *mdx* mice are dilated, hypertrophied, somewhat fibrotic and poorly contracting[4,5,25]. Ventricular cardiomyocytes isolated from senescent but not young *mdx* animals also show signs of dilated cardiomyopathy. The diameter of *mdx* myocytes from old animals is significantly smaller, and their length is significantly greater than of WT cells (in μm: 22.2 ± 0.6 and 127.8 ± 2.4 (n=57) vs 24.7 ± 0.77 and 116.1 ± 2.5 (n=65)), although cell capacitance is not changed (in pF: 239.0 ± 21.2 (n=32) vs 244.5 ± 20.6 (n=32) in *mdx* and WT cells, respectively). Tropnonin I was found to be degraded in dystrophic hearts[21]. In addition, measurements in dystrophic *mdx* papillary muscles revealed that the myofibrillar Ca^{2+} sensitivity is reduced, a finding which contributes to the weak force, in addition to the smaller Ca^{2+} transients[26]. Additionally, electrocardiographic (ECG) deviations such as diminished R- and S-wave amplitudes gradually become apparent in *mdx* mice. By the age of 6 months shortening of the PR interval and polymorphic R-waves suggest disturbances in the cardiac conduction system[27,28].

While in the *mdx* mouse cardiomyopathy only becomes apparent in adulthood, the dystrophin protein is absent throughout the lifetime of the animal. Thus, functional consequences of the lack of dystrophin, such as stress sensitivity, would be expected to be present even in very young and apparently healthy mice. For our study, we focussed on the presently prevailing hypothesis to explain the damages caused by the lack of this protein, which links cytoskeletal proteins with the cell environment: the "Ca^{2+} hypothesis of muscular dystrophy"[29]. This hypothesis proposes that the membrane fragility resulting from the lack of dystrophin leads to extra influx of Ca^{2+} via micro-ruptures and/or stretch activated channels, and that these Ca^{2+} signals are subsequently amplified by CICR and ultimately lead to activation of Ca^{2+} activated proteases, to mitochondrial damage and apoptotic or necrotic cell death. This hypothesis has recently been elaborated to contain another aggravating culprit, excessive oxidative stress.

Our results obtained in cardiomyocytes isolated from young animals now suggest that the oxidative stress is possibly among the very initial problems dystrophic myocytes encounter. In these cells ROS production was already abnormally high. Furthermore, ROS scavengers and inhibitors of NAD(P)H oxidase could prevent most of the acute Ca^{2+} signaling alterations, suggesting NOX as the primary source of this oxidative stress. Why and how NOX becomes abnormally activated in dystrophic cells is not entirely clear and several possibilities exist. For example, NOX over-expression has been reported in dystrophic muscle[21,30]. Activation of NOX could occur indirectly after Ca^{2+} influx, *via* phosphorylation by Ca^{2+} sensitive PKC[31-33]. PKC could also become activated *via* Angiotensin II receptor signaling, which seems to be activated by stretch, even in the absence of an agonist[34]. An activation of NOX by stretch exerted via the intracellular tubulin network has also been suggested[10].

NOX/ROS mediated signaling has a significant downstream impact on Ca^{2+} signaling proteins, and presumably on many other proteins important for cell function. RyRs are not exquisitely susceptible to oxidative modulation. ROS can also turn on CaMKII in a Ca^{2+} independent way[23]. This leads to further RyR sensitization by CaMKII dependent phosphorylation, as observed here with antibodies and with pharmacological CaMKII inhibitors. Taken together, these mechanisms explain the susceptibility of dystrophic cardiomyocytes and their Ca^{2+} signaling system to stress at the very early subclinical phases of the disease.

Our studies further suggest that later during the progression of dystrophic cardiomyopathy, but before heart failure is observed, nitrosation and PKA-dependent phosphorylation contribute to the increased sensitivity of RyRs to Ca^{2+}, in agreement with recently published data[6,19]. At this stage of the disease *mdx* mice as well as DMD patients often exhibit electrocardiographic abnormalities, such as premature ventricular beats. Moreover, during physical or emotional stress CPVTs also have been reported in boys with DMDs[35]. It is possible that under these conditions additional β-adrenergic input may lead to SERCA and I_{Ca}

stimulation, followed by phosphorylation of the RyRs, culminating in a high arrhythmogenic potential due to overloaded SR and hypersensitive RyRs [19].

Finally, our data indicate that at the terminal stages of cardiac dystrophy, several post-translational modifications together hypersensitize RyR to an extent where SR Ca^{2+} leak dramatically increases This may subsequently contribute to cytosolic and mitochondrial Ca^{2+} overload[9,17], activation of necrotic and apoptotic processes and loss of functional myocytes. The latter step usually precedes the development of cardiac fibrosis and reduction in heart contractility[4]. In parallel, enhanced and uncompensated SR Ca^{2+} leak results in a reduction in SR Ca^{2+} load, which will in turn reduce the amplitude of beat to beat intracellular Ca^{2+} transients, thus resulting in reduced force production by the surviving cardiomyocytes. These two cellular processes could eventually impede cardiac contractility leading to cardiac failure.

5. Conclusions.

The present study revealed the gradual time-dependent unfolding of prominent disease pathomechanisms in dystrophic hearts. Our major conclusion is that overall oxidative stress may be more important as one of the early steps of an initial cellular injury than previously thought. We suggest that the "Ca^{2+} hypothesis" of cardiac dystrophy should be significantly modified as it was previously implemented for skeletal muscle disease[36]. Obviously, this view should also be considered when developing new therapies for muscular dystrophy. One can speculate that therapies could even benefit from a combined approach, where oxidative stress and RyR hypersensitivity would be targeted simultaneously.

Funding.

Conflict of interest: none declared.

Figure Legends

Figure 1 Intracellular calcium homeostasis in cardiomyocytes from 1 month old mice *(A)* Intracellular Ca^{2+} responses to mild hypo-osmotic shock in WT and *mdx* cells. Left panels are *XY* images of cardiac myocytes after returning to isotonic solution and line-scan representations of series of images acquired from the cells on the left upon application of an osmotic challenge. Averaged fluorescence was determined within each cell and converted to a two-dimensional X,t image (as in[32]). Bars under the line-scans depict the protocol of extracellular solution changes. Right panel represents pooled data of mean values of normalized fluorescence during 60 sec after the osmotic shock. The averaged response to the osmotic shock was extremely small in WT cells compared to *mdx*. *(B)* Left panels show representative traces of Ca^{2+} currents, line-scan images of Ca^{2+}-related fluorescence and normalized cytosolic transients elicited by a 400 ms test pulse to -25 mV in WT and *mdx* cells superfused with either 1.8 mM or 0.5 mM Ca^{2+}. Line plot on the top represents the voltage protocol used for the experiments. Right panel shows the statistical comparison of EC-coupling gain in 0.5 mM Ca^{2+} in WT and *mdx* cells. For each group, data were normalized to the value of the gain obtained in 1.8 mM Ca^{2+}. SR Ca^{2+} release was much more resistant to the reduction in I_{Ca} trigger in *mdx* myocytes. *(C)* Left panels illustrate intracellular Ca^{2+} signals during the protocol designed to estimate SR Ca^{2+} leak (as in[14]): line-scan images of fluo-3 fluorescence and normalized cytosolic transients. Bars on the bottom depict the protocol of extracellular solution changes. Averaged values of estimated SR Ca^{2+} leak and SR Ca^{2+} load in WT and *mdx* cells are shown at the right. The SR Ca^{2+} leak was determined as a reduction in the resting fluo-3 fluorescence following tetracaine application, expressed as a % of SR Ca^{2+} content estimated from the amplitude of the caffeine-induced SR Ca^{2+} transient. There was no significant difference in the values obtained in WT and *mdx* cells. See Table 1S for details.

Figure 2 Post-translational modifications of RyRs in cells from 1 month old mice *(A)* Representative images of DCF fluorescence in WT and *mdx* myocytes under resting conditions and after application of 10 mM H_2O_2. Graph at the bottom left illustrates changes in the averaged DCF signals. Bar graphs compare the rate of DCF oxidation (slope) at rest and normalized increases in DCF signals after application of H_2O_2 in WT and *mdx* cells . The values were 0.027±0.004 and 0.039±0.003 for the slope and 5.36±0.57 and 7.46±0.64 for F_0/F_{max} in *mdx* and WT cells respectively. Both groups of measurements indicate higher ROS production in *mdx* cells. *(B)* Representative Coomassie-stained gel and mBB fluorescence intensity blot in samples from WT and *mdx* hearts. Bar plot shows averaged data on free thiol content in RyRs from WT myocytes normalized to the corresponding value in *mdx* cells. Level of free thiols is significantly greater in WT hearts. *(C)* Immunoblots and summary of oxidized CaMKII. Band intensities recorded from *mdx* samples were normalized per GAPDH signals and expressed as a percentage of increase compared to values obtained in WT samples. Level of oxidized CaMKII are almost 2 fold higher in *mdx* hearts. *(D)* Immunoblot and summary of phosphorylated RyR. Whereas normalized intensity of CaMKII dependent immunoreactivity increased ~3 fold in dystrophic tissue, the value did not change significantly for the PKA site. Numbers of samples studied are indicated on the bars. *(E)* Reduction in oxidative stress and CaMKII inhibition suppress exaggerated intracellular Ca^{2+} responses to osmotic shock (left panel) and prevent hypersensitivity of EC-coupling (right panel). In the experiments with osmotic shock, individual intracellular Ca^{2+} responses were averaged within each experimental group (e.g. each pharmacological intervention applied) and normalized to the averaged response under control conditions (no drug applied). In the EC-coupling gain experiments, averaged data within each experimental group were also normalized to the values obtained in control (no drug applied) conditions. Details are in Table 1S.

Figure 3 Gradual deterioration of intracellular Ca^{2+} homeostasis during the development of cardiac dystrophy. Intracellular Ca^{2+} responses to osmotic shock *(A)*, gain of EC-coupling *(B)*, intracellular Ca^{2+} leak *(C)* and SR Ca^{2+} content *(D)* in WT and *mdx* cardiomyocytes isolated from 1, 3-4 and 12-15 month old mice. Please note the gradually increased SR Ca^{2+} leak and decreased SR Ca^{2+} load in *mdx* cardiomyocytes from older mice. The corresponding values are listed in Table 2S.

Figure 4 Reduction in oxidative/nitrosative stress as well as CaMKII and PKA inhibition ameliorates excessive intracellular Ca^{2+} responses to osmotic shock and hypersensitivity of EC-coupling in mdx myocytes isolated from 3-4 month old mice *(A and B)* and reduces SR Ca^{2+} leak in cells from mature 12-15 month old mdx mice *(C)*. In the experiments with osmotic shock *(A)*, individual intracellular Ca^{2+} responses were determined as mean values of fluorescence recorded within the cell during 60 s after the shock, then averaged within each experimental group (e.g. each pharmacological intervention applied) and normalized to the averaged response under control conditions (no drug applied). In the EC-coupling gain experiments *(B)*, averaged data within each experimental group were normalized to the values obtained in control (no drug applied) conditions. *(C)* Typical intracellular Ca^{2+} signals measured during the "leak" protocol and averaged values of estimated SR Ca^{2+} leak under control conditions in WT and *mdx* cells and in *mdx* myocytes pretreated with various pharmacological agents (dashed bars). All values are listed in Table 1S.

Figure 5 Signaling pathways involved in regulation of RyR activity in dystrophic cardiomyocytes. The diagram shows the main molecules involved in Ca^{2+} signaling and EC-coupling. Solid lines depict primary (oxidation and CaMKII-phosphorylation) and dashed lines depict secondary (nitrosation and PKA phosphorylation) mechanisms resulting in hypersensitivity of RyRs. Abbreviations CaCh and NaCh refer to L-type Ca^{2+} channel and voltage-gated Na^+ channel,

respectively.

References

1. Hein S, Kostin S, Heling A, Maeno Y, Schaper J. The role of the cytoskeleton in heart failure. *Cardiovasc Res* 2000;**45**:273–278.

2. Durbeej M, Campbell KP. Muscular dystrophies involving the dystrophin-glycoprotein complex: an overview of current mouse models. *Curr Opin Genet Dev* 2002;**12**:349–361.

3. Finsterer J, Stöllberger C. The heart in human dystrophinopathies. *Cardiology* 2003;**99**:1–19.

4. Quinlan JG, Hahn HS, Wong BL, Lorenz JN, Wenisch AS, Levin LS. Evolution of the *mdx* mouse cardiomyopathy: physiological and morphological findings. *Neuromuscul Disord* 2004;**14**:491–496.

5. Stuckey DJ, Carr CA, Camelliti P, Tyler DJ, Davies KE, Clarke K. In vivo MRI Characterization of Progressive Cardiac Dysfunction in the *mdx* Mouse Model of Muscular Dystrophy. *PLoS ONE* 2012;**7**:e28569.

6. Fauconnier J, Thireau J, Reiken S, Cassan C, Richard S, Matecki S, et al. Leaky RyR2 trigger ventricular arrhythmias in Duchenne muscular dystrophy. *Proc Natl Acad Sci U S A* 2010;**107**:1559–1564.

7. Keurs ter HEDJ, Boyden PA. Calcium and Arrhythmogenesis. *Physiol Rev* 2007;**87**:457–506.

8. Yasuda S, Townsend D, Michele DE, Favre EG, Day SM, Metzger JM. Dystrophic heart failure blocked by membrane sealant poloxamer. *Nat Cell Biol* 2005;**436**:1025–1029.

9. Jung C, Martins AS, Niggli E, Shirokova N. Dystrophic cardiomyopathy: amplification of cellular damage by Ca^{2+} signalling and reactive oxygen species-generating pathways. *Cardiovasc Res* 2007;**77**:766–773.

10. Prosser BL, Ward CW, Lederer WJ. X-ROS signaling: rapid mechano-chemo transduction in heart. *Science* 2011;**333**:1440–1445.

11. Ullrich ND, Fanchaouy M, Gusev K, Shirokova N, Niggli E. Hypersensitivity of excitation-contraction coupling in dystrophic cardiomyocytes. *Am J Physiol Heart Circ Physiol* 2009;**297**:H1992–H2003.

12. Wehrens XHT, Lehnart SE, Reiken S, Vest JA, Wronska A, Marks AR. Ryanodine receptor/calcium release channel PKA phosphorylation: a critical mediator of heart failure progression. *Proc Natl Acad Sci U S A* 2006;**103**:511–518.

13. Wolska BM, Solaro RJ. Method for isolation of adult mouse cardiac myocytes for studies of contraction and microfluorimetry. *Am J Physiol* 1996;**271**:H1250–H1255.

14. Shannon TR, Ginsburg KS, Bers DM. Quantitative assessment of the SR Ca^{2+} leak-load relationship. *Circ Res* 2002;**91**:594–600.

15. Huke S, Bers DM. Ryanodine receptor phosphorylation at Serine 2030, 2808 and 2814 in rat cardiomyocytes. *Biochem Biophys Res Commun* 2008;**376**:80–85.

16. Terentyev D, Gyorke I, Belevych AE, Terentyeva R, Sridhar A, Nishijima Y, et al. Redox modification of ryanodine receptors contributes to sarcoplasmic reticulum Ca^{2+} leak in chronic heart failure. *Circ Res* 2008;**103**:1466–1472.

17. Williams IA, Allen DG. Intracellular calcium handling in ventricular myocytes from mdx mice. *Am J Physiol Heart Circ Physiol* 2006;**29**:H846–H855.

18. McCall E, Ginsburg KS, Bassani RA, Shannon TR, Qi M, Samarel AM, et al. Ca flux, contractility, and excitation-contraction coupling in hypertrophic rat ventricular myocytes. *Am J Physiol* 1998;**274**:H1348–H1360.

19. Sarma S, Li N, van Oort RJ, Reynolds C, Skapura DG, Wehrens XHT. Genetic inhibition of PKA phosphorylation of RyR2 prevents dystrophic cardiomyopathy. *Proc Natl Acad Sci U S A* 2010;**107**:13165–13170.

20. Fanchaouy M, Polakova E, Jung C, Ogrodnik J, Shirokova N, Niggli E. Pathways of abnormal stress-induced Ca^{2+} influx into dystrophic mdx cardiomyocytes. *Cell Calcium.* 2009;**46**:114–121.

21. Williams IA, Allen DG. The role of reactive oxygen species in the hearts of dystrophin-deficient mdx mice. *Am J Physiol Heart Circ Physiol* 2007;**293**:H1969–H1977.

22. Xu L, Eu JP, Meissner G, Stamler JS. Activation of the cardiac calcium release channel (ryanodine receptor) by poly-S-nitrosylation. *Science* 1998;**279**:234–237.

23. Erickson JR, Joiner M-LA, Guan X, Kutschke W, Yang J, Oddis CV, et al. A dynamic pathway for calcium-independent activation of CaMKII by methionine oxidation. *Cell* 2008;**133**:462–474.

24. Swynghedauw B. Molecular mechanisms of myocardial remodeling. *Physiol Rev* 1999;**79**:215–262.

25. Zhang W, Hove ten M, Schneider JE, Stuckey DJ, Sebag-Montefiore L, Bia BL, et al. Abnormal cardiac morphology, function and energy metabolism in the dystrophic mdx mouse: An MRI and MRS study. *J Mol Cell Cardiol* 2008;**45**:754–760.

26. Wagner S, Knipp S, Weber C, Hein S, Schinkel S, Walther A, et al. The heart in Duchenne muscular dystrophy: early detection of contractile performance alteration. *J Cell Mol Med* 2012; doi: 10.1111/j.1582-4934.2012.01630.x. [Epub ahead of print].

27. Bia BL, Cassidy PJ, Young ME, Rafael JA, Leighton B, Davies KE, et al. Decreased myocardial nNOS, increased iNOS and abnormal ECGs in mouse models of Duchenne muscular dystrophy. *J Mol Cell Cardiol* 1999;**31**:1857–1862.

28. Chu V, Otero JM, Lopez O, Sullivan MF, Morgan JP, Amende I, et al. Electrocardiographic findings inmdx mice: a cardiac phenotype of Duchenne muscular dystrophy. *Muscle Nerve* 2002;**26**:513–519.

29. Deconinck N, Dan B. Pathophysiology of duchenne muscular dystrophy: current hypotheses. *Pediatr Neurol* 2007;**36**:1–7.

30. Shkryl VM, Martins AS, Ullrich ND, Nowycky MC, Niggli E, Shirokova N. Reciprocal amplification of ROS and Ca^{2+} signals in stressed mdx dystrophic skeletal muscle fibers. *Pflugers Arch* 2009;**458**:915–928.

31. Jiang F, Zhang Y, Dusting GJ. NADPH oxidase-mediated redox signaling: roles in cellular stress response, stress tolerance, and tissue repair. *Pharmacol Rev* 2011;**63**:218–242.

32. Martins AS, Shkryl VM, Nowycky MC, Shirokova N. Reactive oxygen species contribute to Ca^{2+} signals produced by osmotic stress in mouse skeletal muscle fibres. *J Physiol* 2008;**586**:197–210.

33. Gul R, Shawl AI, Kim SH, Kim UH. Cooperative interaction between reactive oxygen species and Ca^{2+} signals contributes to angiotensin II-induced hypertrophy in adult rat cardiomyocytes. *Am J Physiol Heart Circ Physiol* 2012;**302**:H901–H909.

34. Zhou C. Angiotensin II and Stretch Activate NADPH Oxidase to Destabilize Cardiac Kv4.3 Channel mRNA. *Circ Res* 2006;**98**:1040–1047.

35. Hermans MCE, Pinto YM, Merkies ISJ, de Die-Smulders CEM, Crijns HJGM, Faber CG. Hereditary muscular dystrophies and the heart. *Neuromuscul Disord* 2010;**20**:479–492.

36. Rando TA. Role of nitric oxide in the pathogenesis of muscular dystrophies: a "two hit" hypothesis of the cause of muscle necrosis. *Microsc Res Tech* 2001;**55**:223–235.

Fig. 1.

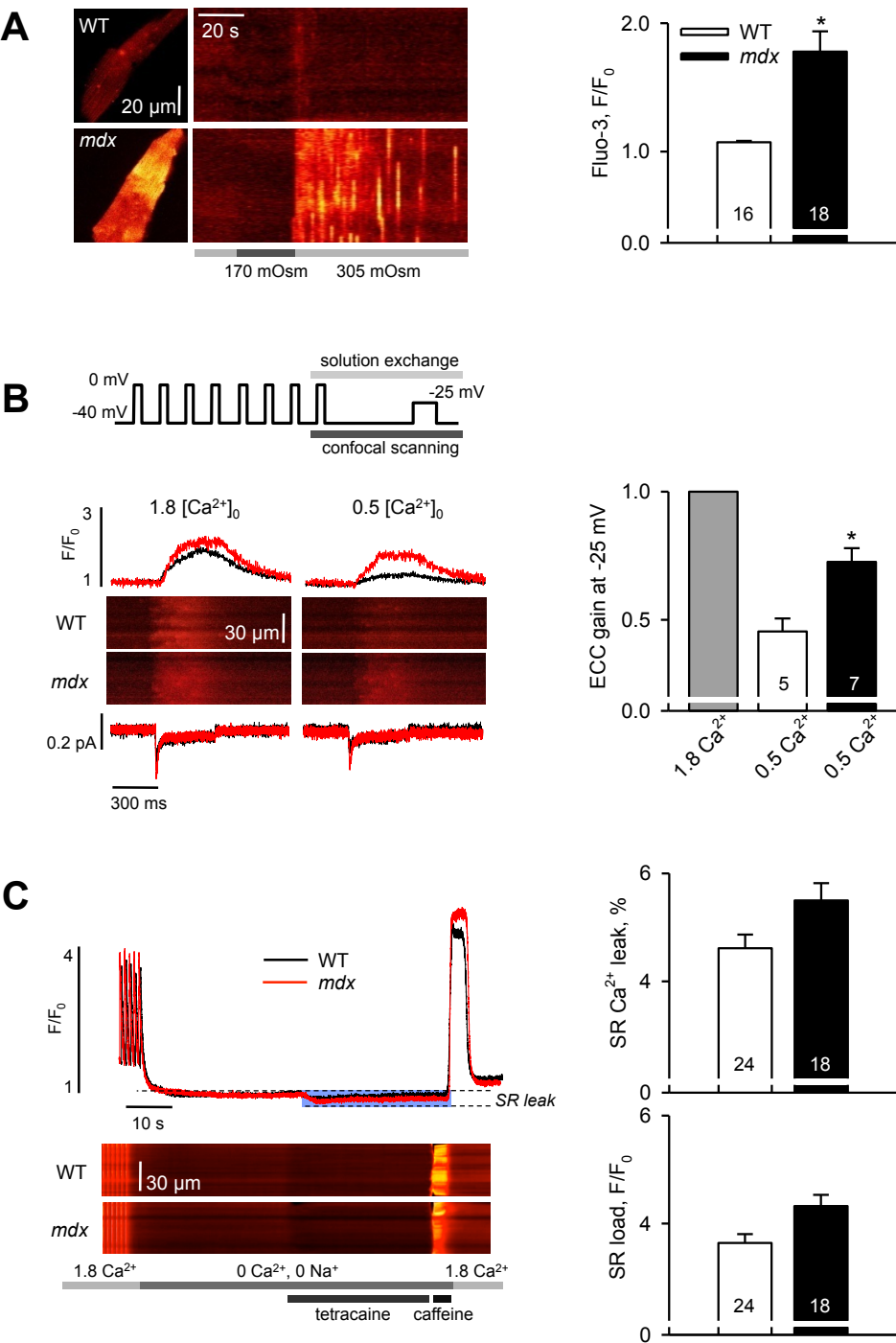Fig. 2.

A

young   adult   senescent

*

*   *

Fluo-3, F/F$_0$

2.4

1.6

0.8

0.0

24   18   8   18   17   16

B

young   adult   senescent

*

*

*

ECC gain at -25 mV

2

1

0

5   7   7   9   6   10

1.8 Ca^{2+} 0.5 Ca^{2+}

C

young   adult   senescent

*

*

SR Ca^{2+} leak, %

8

6

4

24   18   8   18   17   16

☐ WT
■ *mdx*

D

young   adult   senescent

SR load, F/F$_0$
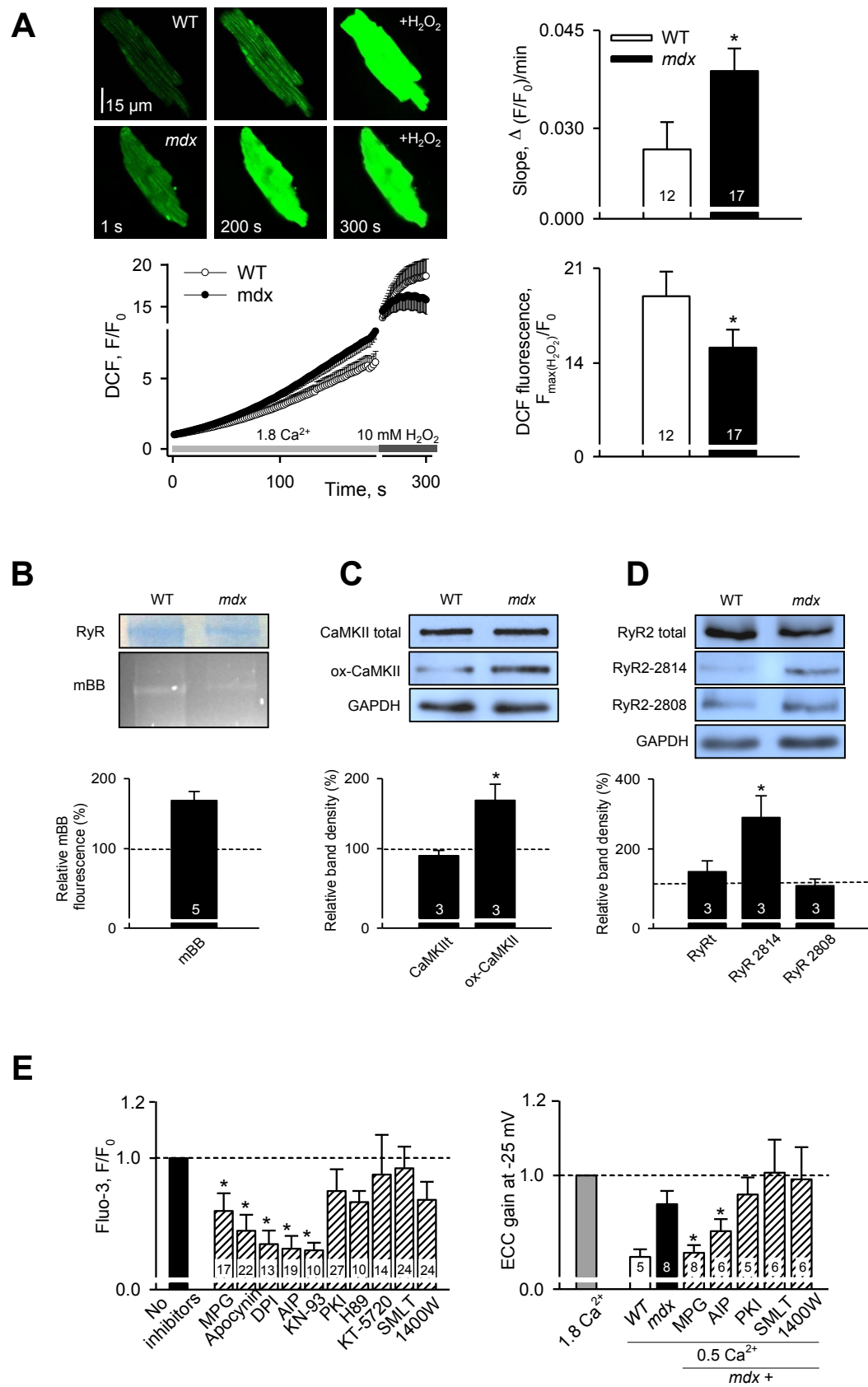
6

4

24   18   8   18   17   16
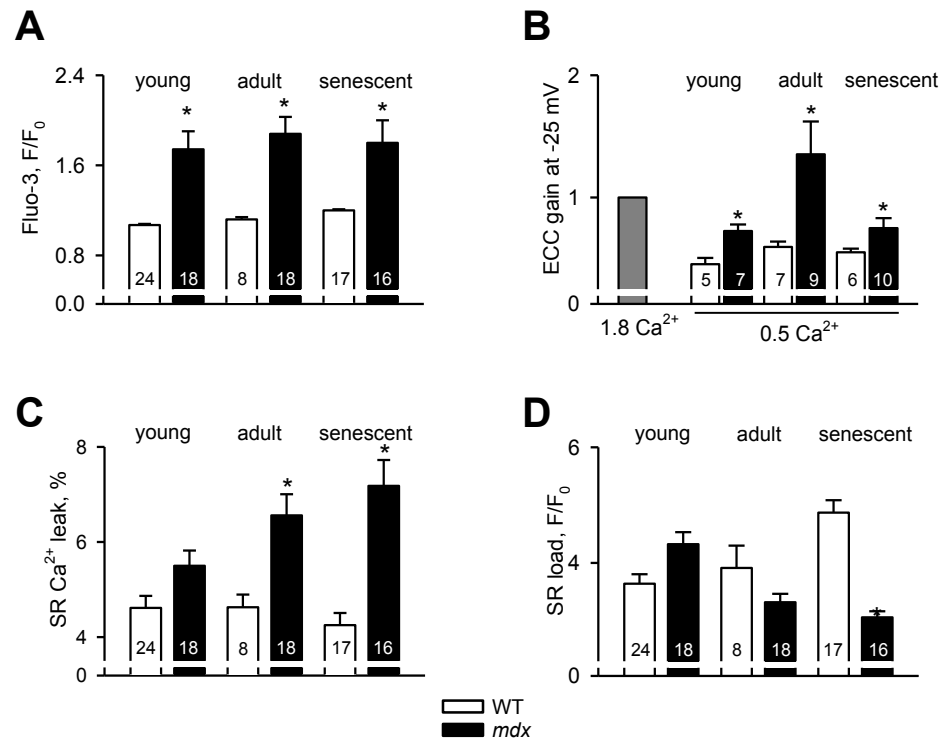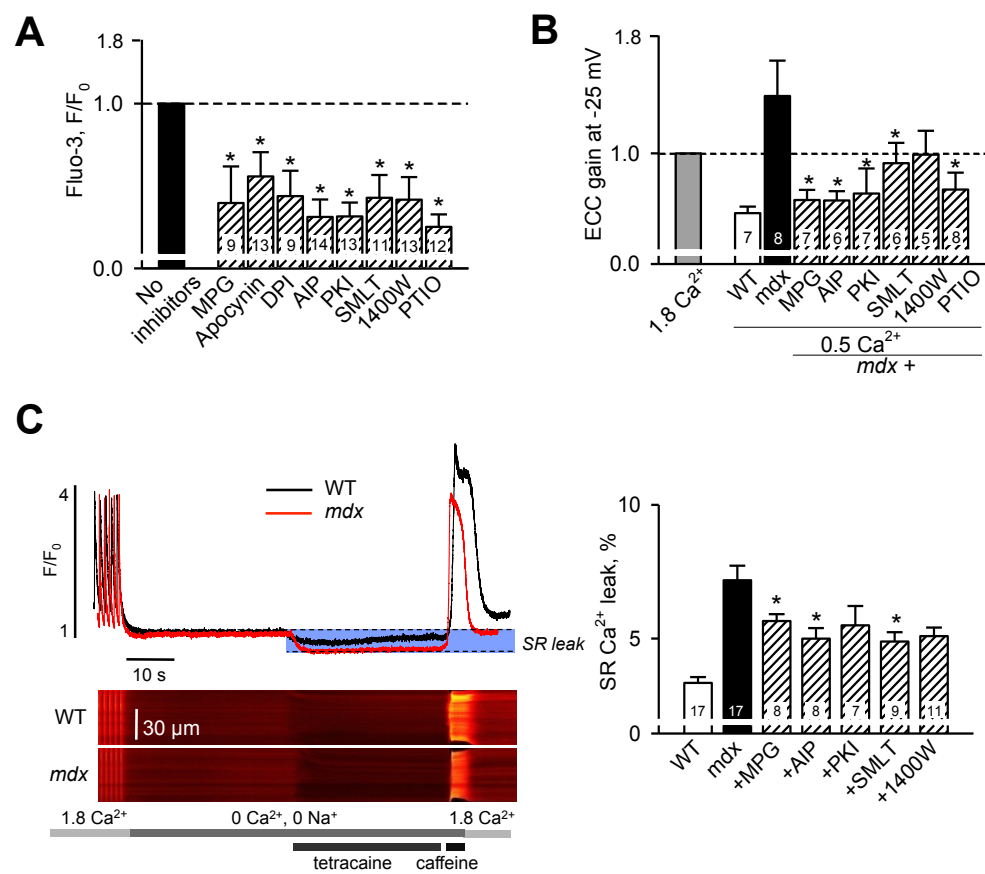
Fig. 3.

Fig. 4.

Fig.5

Supplementary Materials

Methods.

Cell Isolation. C57BL10 mice (wild-type, WT) and dystrophin-deficient *mdx* (C57BL/10ScSn-*mdx*) mice at the age of 1 (young), 3-4 (adults) and above 12-15 months old (senescent) were used in this study. Animals were purchased from the Jackson Laboratory. Ventricular myocytes from mouse heart were isolated as previously described[1]. Briefly, hearts were excised, cannulated and retrogradely perfused with (in mM): 140 NaCl, 5.4 KCl, 1.1 $MgCl_2$, 1 Na_2HPO_4, 5 HEPES and 10 glucose, pH was adjusted to 7.3 with NaOH at 37^0C. Cells were enzymatically dissociated with collagenase type II (Worthington) and protease (Sigma) treatment and used within 4-5 hours. All experiments were performed at room temperature and conformed with the National Institutes of Health Guide for the Care and Use of Laboratory Animals (1996) and were approved by the Institutional Animal Care and Use Committee of the New Jersey Medical School of the University of Medicine and Dentistry of New Jersey and by the State Veterinary Office of Bern, Switzerland.

Intracellular Ca^{2+} responses to hypo-osmotic shock. Intact cardiomyocytes were loaded with fluo-3 AM (5 μM, Biotium) for 30 min at room temperature followed by at least 10 min of de-esterification. Cytosolic Ca^{2+} transients were recorded with fluo-3 and a laser scanning confocal microscope (Bio-Rad, Radiance 2000) in *XY*-scan mode at at the rate of 1 frame per 2 seconds. Fluo-3 was excited with the 488 nm line of an Argon laser and emission above 500 nm was collected. As a rule, 100 images were acquired: 10 images were taken in isotonic solution contained (in mM): 140 NaCl, 4 KCl, 1.8 $CaCl_2$, 1.1 $MgCl_2$, 10 glucose, 5 HEPES (further referred to as NT). Osmolarity was 305 mOsm and pH was adjusted to 7.4 with NaOH. Then 20 images were recorded in hypoosmotic solutions which contained 70 NaCl (instead of 140 NaCl) and consequently reduced osmolarity of 170 mOsm and the remaining 70 frames were recorded back in isotonic solution. The averaged intracellular Ca^{2+} responses during 60 sec after the osmotic shock were compared in different series of experiments.

Excitation-contraction coupling (electrophysiological recordings combined with confocal imaging). Membrane currents were measured using the whole cell patch-clamp procedures with an Axopatch 200B amplifier (Axon Instruments) controlled by custom-written data-acquisition software developed under LabView (National Instruments). Cells were voltage clamped using low-resistance (1.5–3 MΩ) borosilicate glass micropipettes pulled with a Zeitz DMZ puller (Zeitz Instruments, Germany) and filled with pipette solution which contained (in mM): 120 CsAsp, 8 NaCl, 20 tetraethylammonium (TEA)-Cl, 5.5 $MgCl_2$, 4 KATP, 5 HEPES, and 0.1 K_5-fluo-3. pH was adjusted to 7.2 with CsOH and osmolarity was 305 mOsm. Cells were held at -80 mV. After eight preconditioning pulses to 0 mV in order to equalize the SR Ca^{2+} load, a 400 ms test pulse to -25 mV was applied after an initial step to -40 mV to inactivate Na^+ and T-type Ca^{2+} currents. The SR loading protocol was applied in NT (with 1.8 $CaCl_2$) with a rapid switch to NT (with 0.5 $CaCl_2$) before the last preconditioning pulse. Simultaneously with Ca^{2+} currents intracellular Ca^{2+} transients were recorded in line-scan mode at a rate 750 lines/sec. The E-C coupling gain was calculated from the ratio of peak Ca^{2+} transients and peak Ca^{2+} currents at several tested clamp potentials and compared at different external Ca^{2+} concentrations

Estimation of SR Ca^{2+} leak. SR Ca^{2+} leak was estimated as described in[2]. Cells were paced at 1 Hz in external control solution to obtain steady-state levels of SR Ca^{2+} load, and starting from the last five beats, $[Ca^{2+}]_i$ was recorded in the line-scan mode (500 lines/s). After pacing, external solution was rapidly switched to Na$^+$ and Ca^{2+}-free solution (by substitution of Na$^+$ with Li$^+$ and addition of 0.5 mM EGTA) for 15 s to stop Ca^{2+} influx and to inhibit Ca^{2+} removal via the NCX and thus, to avoid Ca^{2+} overload of the cells. Addition of tetracaine (1 mM, 15 s) eliminated RyR-mediated diastolic Ca^{2+} leak, leading to a rapid decrease in $[Ca^{2+}]_i$ proportionally to the leak. The peak of the caffeine-induced Ca^{2+} transient measured after tetracaine washout (10 mM caffeine, 2 s) was used to estimate SR load.

Measurements of cytosolic ROS production and RyR free thiol content. For the quantification of ROS production, cells were loaded with 20 μM of 5-(and-6)-chloromethyl-20 , 70-dichlorodihydrofluorescein diacetate (CM-H$_2$DCFDA, Invitrogen). CM-H$_2$DCFDA is hydrolysed to DCFH in the cell, and DCFH is oxidized to form highly fluorescent DCF in the presence of the appropriate oxidant (e.g. hydrogen peroxide or peroxynitrite). ROS/RNS generation was detected as a result of DCFH oxidation. As a rule, a series of 160 images was acquired at 0.5 Hz. CM-H2DCFDA was excited at 488 nm of Argon laser and emission was collected above 500 nm. Laser power was minimized to reduce the photoproduction of ROS. At the end of each experiment 10 mM H$_2$O$_2$ was added to determine maximum DCF fluorescence. The content of free thiols in RyR was determined using monobromobimane (mBB) fluorescence assay as described in[3]. Isolated cardiomyocytes were permeabilized, incubated with 1 mM of mBB for 1 hour in dark room and washed out 3 times to remove unbound mBB. The proteins were resolved in the 4-15% TGX SDS-gels (Bio-rad, CA) and transilluminated with UV light (excitation wavelength 360nm) by using MultiImage™ light cabinet (Alpha innotech, CA). Total RyR2 was determined from Coomassie blue staining of the gels run in parallel and confirmed by western blotting with anti-RYR2 (Thermo Scientific, MA).The location of the RyR band on this gel was also reassured with Mass Spectrometry at UMDNJ core facility.

Phosphorylation and Western Blots of RyR.
Mouse ventricular tissue was collected and sonicated in the radio-immunoprecipitation assay (RIPA) lysis buffer (1X TBS, 1% P-40, 0.5% sodium deoxycholate, 0.1% SDS, 0.004% sodium azide supplemented with phenylmethylsulfonyl fluoride PMSF, protease inhibitor cocktail and Calyculin A (Santa Cruz, CA)). Protein concentration in each sample was determined using an Eppendorf photometer with bovine serum albumin (BSA) as a standard. For immunoblotting, 40 µg of protein lysate per sample was denatured in 4X SDS-PAGE sample loading buffer. Proteins were separated by electrophoresis in to 4% (for RyR 2) and 10% (for CaMKII) respectively SDS-polyacrylamide gel, transferred to nitrocellulose membrane (Bio-Rad, CA) at 15V for 16-18 h at 4^{0}C (for RyR2) and at 90V for 15 h at 4^{0}C (for CaMKII), blocked with 1% BSA in TRIS buffered saline and Tween (TBS: 20mM TRIS-HCl, 200mM NaCl, 0.6% tween 20, pH 7.5) for 1 hour and probed for proteins of interest. Levels of RyR2, phosphorylated-RyR2, CaMKII and oxidized-CaMKII were assessed using specific primary antibodies: anti-RyR2 (1:500, Thermo Scientific, USA), anti-phosphorylated-RyR2-2808 (1:2000, Badrilla, UK), anti-phosphorylated-RyR2-2814 (1:500, Badrilla, UK), anti-CaMKII and anti-oxidized-CaMKII (1:500, both are a gift from Dr. M. Anderson) and appropriate HRP-conjugated secondary antibodies. Membranes were washed 3 times for 15 min in TBST after primary antibodies and secondary antibodies incubation respectively.The chemiluminescence was detected and acquired on to MultiImage™ light cabinet (Alpha Innotech, USA). GAPDH (1:1000, Millipore, USA) was probed as a protein loading control.

Data analysis and statistics. Images were pre-processed using the free software NIH ImageJ and further analyzed, together with electrophysiological data, in IgorPro Software (Wavemetrics). Results are shown as mean ± standard error of mean (SEM). All data sets contain results from a minimum of three mice (n on the bars indicates the number of cells). Statistical significance was evaluated by Student's t-test. A P-value of <0.05 was considered significant. On the graphs the significance is indicated by *.

1. Wolska BM, Solaro RJ. Method for isolation of adult mouse cardiac myocytes for studies of contraction and microfluorimetry. *Am J Physiol* 1996;**271**:H1250–1255.

2. Shannon TR, Ginsburg KS, Bers DM. Quantitative assessment of the SR Ca^{2+} leak-load relationship. *Circ Res* 2002;**91**:594–600.

3. Terentyev D, Gyorke I, Belevych AE, Terentyeva R, Sridhar A, Nishijima Y *et al.* Redox modification of ryanodine receptors contributes to sarcoplasmic reticulum Ca^{2+} leak in chronic heart failure. *Circ Res* 2008;**103**:1466–1472.

Table I. Pharmacology of Ca^{2+} signaling in *mdx* cardiomyocytes.

Ca^{2+} responses to osmotic shock, F/F$_0$				
Inhibitor	**Young (control)**	**Young (+inhibitor)**	**Adult (control)**	**Adult (+inhibitor)**
MPG	1.67 ± 0.13 (21)	1.36 ± 0.10 (17)	1.93 ± 0.18 (10)	1.33 ± 0.22 (9)
Apocynin	2.01 ± 0.18 (18)	1.50 ± 0.11 (22)	1.66 ± 0.13 (12)	1.28 ± 0.13 (13)
DPI	1.74 ± 0.12 (20)	1.21 ± 0.08 (13)	2.01 ± 0.15 (18)	1.43 ± 0.16 (9)
AIP	2.03 ± 0.15 (24)	1.38 ± 0.09 (24)	2.02 ± 0.15 (11)	1.30 ± 0.11 (11)
KN-93	1.65 ± 0.22 (13)	1.11 ± 0.04 (10)		
PKI	1.76 ± 0.09 (27)	1.56 ± 0.13 (24)	1.79 ± 0.17 (21)	1.16 ± 0.08 (13)
H89	1.56 ± 0.23 (16)	1.10 ± 0.15 (24)		
KT-5720	1.60 ± 0.31 (11)	1.44 ± 0.05 (10)		
SMLT	1.76 ± 0.16 (15)	1.69 ± 0.13 (19)	2.10 ± 0.19 (14)	1.48 ± 0.15 (14)
1400W	1.92 ± 0.14 (24)	1.70 ± 0.12 (27)	2.08 ± 0.15 (17)	1.45 ± 0.15 (13)
EC-coupling gain @-25 mV @0.5 Ca^{2+}, (ΔF/F$_0$)/(A/F)				
Inhibitor	**Young (control)**	**Young (+inhibitor)**	**Adult (control)**	**Adult (+Inhibitor)**
MPG		0.48 ± 0.05 (8)		1.39 ± 0.24 (7)
AIP		0.63 ± 0.08 (6)		0.68 ± 0.07 (6)
PKI	0.81 ± 0.09 (8)	0.87 ± 0.11 (5)	1.38 ± 0.27 (8)	0.73 ± 0.17 (7)
SMLT		1.02 ± 0.22 (6)		0.93 ± 0.14 (6)
1400W		0.97 ± 0.22 (6)		0.99 ± 0.16 (5)
PTIO#				0.75 ± 0.11 (8)
SR Ca^{2+} Leak, %				
Inhibitor	**Senescent (control)**	**Senescent (+Inhibitor)**		
MPG		5.66 ± 0.25 (8)		
AIP		4.99 ± 0.39 (8)		
PKI	7.18 ± 0.54 (17)	5.49 ± 0.72 (7)		
SMLT		4.89 ± 0.35 (9)		
1400W		5.09 ± 0.32 (11)		

#NO scavenger PTIO (2-Phenyl-4,4,5,5-tetramethylimidazoline-1-oxyl 3-oxide, 0.1 mM) was used to confirm results with NOS inhibitors.

Table II. Gradual deterioration of Ca^{2+} signaling in *mdx* cardiomyocytes.

	Young		Adult		Senescent	
	WT	***mdx***	**WT**	***mdx***	**WT**	***mdx***
Ca^{2+} responses to osmotic shock, F/F$_0$						
	1.07 ± 0.01 (n=24)	1.74 ± 0.16 (n=18)	1.12 ± 0.02 (n=8)	1.88 ± 0.15 (n=18)	1.20 ± 0.01 (n=17)	1.80 ± 0.20 (n=16)
EC-coupling gain @-25 mV @0.5 Ca^{2+}, (ΔF/F$_0$)/(A/F)						
	0.45 ± 0.05 (n=5)	0.73 ± 0.05 (n=7)	0.60 ± 0.04 (n=7)	1.35 ± 0.27 (n=9)	0.55 ± 0.03 (n=6)	0.75 ± 0.08 (n=10)
SR Ca^{2+} Leak, %						
	4.61 ± 0.25 (n=24)	5.50 ± 0.32 (n=18)	4.63 ± 0.27 (n=8)	6.56 ± 0.45 (n=18)	4.25 ± 0.26 (n=17)	7.18 ± 0.54 (n=16)
SR Ca^{2+} Load, F/F$_0$						
	3.64 ± 0.16 (n=24)	4.32 ± 0.21 (n=18)	3.91 ± 0.39 (n=8)	3.32 ± 0.15 (n=18)	4.87 ± 0.21 (n=17)	3.06 ± 0.10 (n=16)